Bull. Mater. Sci., Vol. 34, No. 2, April 2011, pp. 327–335. © Indian Academy of Sciences.

Aqueous slip casting of $MgAl_2O_4$ spinel powder

IBRAM GANESH
Centre for Advanced Ceramics, International Advanced Research Centre for Powder Metallurgy and New Materials (ARCI), Hyderabad 500 005, India

MS received 13 January 2009

Abstract. A stoichiometric $MgAl_2O_4$ spinel (MAS) powder was synthesized by calcining a compacted mixture of α-Al_2O_3 and calcined caustic MgO at 1400°C for 1 h and was surface treated against hydrolysis using an ethanol solution of H_3PO_4 and $Al(H_2PO_4)_3$ after fine grinding. Aqueous suspensions with 41–45 vol.% treated powder were prepared using tetra methyl ammonium hydroxide (TMAH) and an ammonium salt of polyacrylic acid (Duramax D-3005) as dispersing agents. These stable suspensions were consolidated in plaster moulds by slip casting (SC) route for the first time. For comparison purposes, the treated powder was also compacted by die-pressing technique after converting into freeze-dried granules and sintered along with slip cast samples at 1550–1650°C for 1–2 h. The MAS ceramics fabricated by slip casting and die-pressing exhibited comparable properties.

Keywords. $MgAl_2O_4$ spinel; phosphate coating; aluminium dihydrogen phosphate; orthophosphoric acid; slip casting; freeze granulation; double-stage firing process.

1. Introduction

Magnesium aluminate ($MgAl_2O_4$) spinel (MAS) possesses many important thermal, chemical, mechanical and physical properties (Hing 1976; Green *et al* 1989; Baudin *et al* 1995; Sainz *et al* 1995). Furthermore, it does not react with SiO_2 until 1735°C, with MgO or CaO until 2000°C, with Al_2O_3 until 1925°C and, except alkaline earth metals, it can be in contact with all other metals (Belding and Letzgus 1976). Owing to these properties, MAS has been employed for various purposes such as an optical system for pressure vessels, bullet proof vehicles, IR window and dome applications (Harris 1992; Patel *et al* 2000; Wei 2005) and as a humidity sensor (Shimizu *et al* 1985), an alternative material to replace the conventional carbon anode in aluminium electrolytic cells (Angappan *et al* 2004), and an effective refractory material for cement rotary kilns and steel ladles (Urita *et al* 1993; O'Driscoll 1997; Ganesh *et al* 2002a). Recently, it has also been considered as an attractive matrix material for ceramic-matrix composites because of its good chemical compatibility with alumina, zirconia, and mullite ceramics. In spite of these advantages, this material suffers from a problem of volume expansion (~8%) associated with its phase formation from alumina and magnesia (Nakagawa *et al* 1995). Due to this problem, dense MAS ceramics cannot be prepared following a single-stage reaction sintering process (Ganesh *et al* 2005, 2008a). Alternatively, the compacted mixture of alumina and magnesia raw materials are initially calcined at about 1400°C to obtain powder with a spinel content of >90%, followed by fine grinding, compaction, and sintering at >1650°C to form dense ceramics. Due to the involvement of two firing cycles, the cost of production of these ceramics has been increased considerably.

Furthermore, when hollow or complex shaped parts are to be produced, colloidal consolidation techniques appear as the most appropriate. However, the basic nature of MAS powder makes the preparation of aqueous suspensions difficult because this powder undergoes hydrolysis that tend to coagulate the slurries, limiting the practical solids loading to about 30 vol.%, especially when the deagglomeration process by ball milling is conducted for more than 2 h. Due to these reasons, it is rather difficult to obtain stable and concentrated aqueous MAS suspensions to be used in the near-net shape forming of ceramics following colloidal processing techniques. In fact, near-net-shaping is of great importance because expensive post-sintering machining operations can be minimized or even eliminated, reducing the cost of production considerably (Janney *et al* 1998). Besides these advantages, aqueous processing offers several environmental and economic benefits apart from the ability to manipulate inter-particle forces in aqueous suspensions. The existing near-net-shape forming techniques include gel-casting (Janney *et al* 1998; Ganesh *et al* 2008b), hydrolysis assisted solidification (Kosmac *et al* 1997), hydrolysis-induced aqueous gel-casting (Ganesh 2009), direct coagulation casting (Graule *et al* 1994), and temperature-induced forming (Bergström 1994). Since, the fracture in the ceramic materials originates on microstructural imperfections such as pores and inclusions causing poor mechanical reliability, an effective deagglomeration of the powder particles in the

(ibramganesh@arci.res.in)

suspensions is very essential, which is difficult to achieve in the case of aqueous MAS suspensions.

In view of the above problems, at present MAS components for infrared dome and radome (missile) applications are being fabricated by hot isostatic pressing (~1500°C and 200–400 MPa pressure) followed by extensive (and expensive) machining to obtain the desired final shape (Harris 1992; Patel *et al* 2000; Wei 2005). Alternatively, the cold iso-static pressing (CIPing) and freeze casting/consolidation (FC) techniques were also employed for fabricating near-net shape components, which would minimize the cost of production (Urita *et al* 1993; O'Driscoll 1997). The advantages of these processes over hot-pressing technique are low cost of production due to the involvement of ambient conditions, the use of inexpensive materials (aluminium or steel) for mould fabrication, and minimum post-sintering machining operations. Furthermore, these ceramics were found to have minimal residual stresses. However, the product yield of these processes was found to be not encouraging and the mechanical strength of the green consolidates was poor.

Recently, a pressure-less molten metal infiltration technique has also been employed for the fabrication of these components with near-net shape (Kumar and Sandhage 1998). In this process, initially, the molten Mg is infiltrated into porous (65–70% dense) Al_2O_3 preforms at 680–700°C. After solidification, the Mg–Al_2O_3-bearing precursors are oxidized in flowing oxygen at 430°C for 40 h or 700°C for 6 h. The mixtures of MgO and Al_2O_3 thus obtained are further annealed in oxygen at 1200°C for 15 h to obtain MAS material, which is further sintered for 10 h at 1700°C in flowing Ar to achieve a maximum density of about 92·5% of the theoretical. The linear shrinkage upon firing was about 0·6%. However, these products are not suitable for many of the applications due to their low density.

Considering the suitability of aqueous colloidal shaping techniques for the fabrication of IR domes and windows for strategic applications, we have undertaken a systematic study, and successfully prepared stable aqueous MAS suspensions that could be slip cast into components with near-net shape. Initially, a stoichiometric MAS powder was synthesized by solid state reaction at 1400°C for 1 h from a compacted stoichiometric mixture of α-Al_2O_3 and MgO (Ganesh *et al* 2009). This powder was surface-treated in an ethanol solution containing orthophosphoric acid (H_3PO_4) and aluminium di-hydrogen phosphate [$Al(H_2PO_4)_3$] (Ganesh *et al* 2008c). The treated powder could easily be dispersed to obtain stable aqueous suspensions with 41–45 vol.% solids loading and used for slip casting. For comparison purposes, the surface-treated MAS powder was also die-pressed after converting into granules by freeze granulation technique. The differently consolidated samples were sintered for 1–2 h at 1550–1650°C and thoroughly characterized for bulk density, apparent porosity, water absorption capacity, microstructure, XRD phase, hardness, and flexural strength in order to evaluate the effects of processing parameters on the shape forming capability and densification ability of MAS powder.

2. Experimental

2.1 *Synthesis of MAS powder*

A stoichiometric precursor powder mixture of alumina (CT-3000SG, Alcoa-Chemie GmbH, Ludwigshafen, Germany, average particle size, 1·84 μm, BET SSA, 4·06 m^2/g) and calcined caustic magnesia (José M. Vaz Pereira, S.A., Porto, Portugal, average particle/agglomerate size, 5·63 μm, BET SSA, 15·15 m^2/g) was dispersed in an azeotropic mixture of 60 vol.% methyl-ethyl-ketone (MEK) (Honeywell, Riedel-de Haen, Hanover, Germany) and 40 vol.% absolute ethanol (E) (Merck, Darmstadt, Germany) with the help of Hypermer KD1 (a polyester/polyamine copolymer having an estimated MW of about 10000 g/mol, Imperial Chemical Industries PLC, London, UK) to achieve about 40 vol.% solids loading in the suspension. The resultant suspension was deagglomerated for 24 h in polypropylene bottle using alumina balls (12 mm diameter) by maintaining 1:3 weight ratio between powder and balls. The homogenized suspension was separated from the alumina balls and then transferred to a glass beaker, which was placed in a refrigerator (Whirlpool 310 Deluxe, Whirlpool, Madrid, Spain) at −5°C. The consolidated mass was evacuated under a pressure of 1×10^{-1} torr using a turbo pump (98·93 l per min capacity, Model: 949–9315, Varian DS-102; Torino, Italy) at −5°C and further dried at about 40°C in an electric hot-air oven. The gelation mechanism involved in this process was mainly based on the cooling up of dissolved dispersant molecules, inducing *in situ* gelation (i.e., TIG) and the formation of a rigid network bridging the suspended particles (Bergström 1994). The dried mass was calcined in an electrically heated open-air muffle furnace for 1 h at 1000–1400°C to obtain a stoichiometric MAS powder (Ganesh *et al* 2001, 2002b, 2003, 2004). The MAS powder was then crushed, ground in an hammer mill (Retsch GmbH, model SK1, Haan, Germany) and planetary ball milled (Retsch GmbH, PM400, Haan, Germany) at 200 rpm for 3 h in an absolute ethanol. The solids loading in the slurry was 30 vol.% and the powder to balls weight ratio was 1:3. Henceforth, this milled powder, with a BET SSA of 3·98 m^2/g, is termed as A-MAS (as-milled) powder.

2.2 *Surface treatment of MAS powder*

In a typical experiment, 268·5 g A-MAS powder was suspended in 250 mL absolute ethanol in a 500 mL volume three neck round bottom (RB) flask. The RB flask was fitted with an equalization funnel and valve to pass dry-nitrogen gas, and was placed into a thermostatic oil bath (150 mm diameter and 75 mm height, Thermol-100, Biolabs, Hyderabad, India, −50° to +250°C). In a separate experiment, 2 g of

$Al(H_2PO_4)_3$ (assay ≥97·0%, Fluka, Seelze, Germany) was digested in 5 mL of hot H_3PO_4 (85% assay, AR Grade, Qualigens, Mumbai, India). This solution was then mixed with 50 mL ethanol and added drop-by-drop to the above alcohol-based MAS suspension with the help of an equalization funnel. The RB flask was then continuously refluxed at 80°C for 24 h while passing N_2 at the rate of 100 mL/min (Ganesh *et al* 2008c). The contents of the RB were agitated with a magnetic stirrer (5MLH-DX, Remi, Hyderabad, India). The treated MAS slurry was filtered off and washed with fresh ethanol several times in order to remove the excess of H_3PO_4 and $Al(H_2PO_4)_3$. After distillation, the ethanol was reused several times for washing the treated powder. This treated powder is henceforth referred to as T-MAS.

2.3 *Powder processing*

Aqueous suspensions with 41–45 vol.% solids loading were prepared by dispersing the T-MAS powder in deionized water with the help of 25 wt.% aqueous TMAH (Fluka, Seelze, Germany) and Duramax D-3005 (polyacrylic acid ammonium salt, a cationic dispersing agent, Rohm and Haas, Lauterbourg, France) employed at the ratio of 35 μL and 30 μL per gram of powder, respectively. The above suspensions were ball milled for 24 h in polypropylene bottles using alumina balls (12 mm diameter) by maintaining 1:3 weight ratio between powder and balls. After removing the balls, the suspensions were degassed for 5 min by vacuum pumping to evacuate the air bubbles. Afterwards, the suspensions were cast into plaster moulds, which were then allowed under ambient conditions to set and dried at about 40°C for 12 h followed by drying at 90°C for further 12 h. Slip cast green crucibles obtained from a suspension containing 45 vol.% solids loading are shown in figure 1.

For comparison purposes, the treated powder was also compacted by die-pressing of freeze dried granules under a pressure of 200 MPa in a metal die to obtain pellets with 30 mm diameter and ∼8 mm height. It is well known that deagglomeration of powder particles in a suspension is easier at moderate-high solids loading in comparison to diluted suspensions. On the other hand, concentrated suspensions tend to exhibit shear thickening characteristics when submitted to high shear rates as those prevailing upon passing through a narrow (0·7 mm diameter) spraying nozzle. Because of these reasons, the suspensions were diluted to 35 vol.% prior to freeze granulation by adding the required amount of distilled water and 3 wt.% on powder weight basis of an emulsion binder, Duramax D-1000 (Rohm and Haas, Lauterbourg, France). Freeze granulation was performed by spraying the suspensions into liquid nitrogen (−196°C) (Power Pro freeze granulator LS-2, Gothenburg, Sweden). The resultant granules were then dried at −49°C under a pressure of 1×10^{-3} torr in a freeze drying system (Labconco, LYPH Lock 4·5, Kansas City, USA) for several days. The dried granules were uniaxially pressed in a metal die by applying a pressure of 200 MPa to obtain pellets having 30 mm diameter and 8 mm height. The die-pressed and slip cast MAS bodies were subjected to binder removal at 500°C for 2 h and then sintered for 1–2 h at 1550–1650°C.

2.4 *Characterization of powders, suspensions and sintered bodies*

A Gemini Micromeritics BET surface area analyzer (Model 2360, Micromeritics, Norcross, GA, USA) was used for

Figure 1. Green $MgAl_2O_4$ spinel crucibles consolidated by aqueous slip casting from a suspension containing 45 vol.% solids loading.

surface area measurements of the powders. Surface area was measured by nitrogen physisorption at liquid nitrogen temperature (−196°C) by taking 0·162 nm^2 as the area of cross section of N_2 molecule. Particle size analysis of the powders was performed by using light scattering equipment (Coulter LS 230, UK, Fraunhofer optical model). The viscosity of suspensions was measured using a rotational Rheometer (Bohlin C-VOR Instruments, Worcestershire, UK). The measuring configuration adopted was a cone and plate (4°, 40 mm, and gap of 150 μm), and flow measurements were conducted between 0·1 and 800 s^{-1}. The zeta-potentials of powders in 10^{-3} M KCl aqueous solutions were measured on a zeta meter (Delsa 440 Sx, Coulter, Buckinghamshire, UK). Dilute HNO_3 (AR Grade, Qualigens, Mumbai, India) and TMAH solutions were used for pH adjustment. Stock suspensions containing 5 wt.% of ball-milled (24 h) powder were prepared without and with different added amounts of TMAH, Duramax D-3005, or their mixtures. Particulates and supernatant were separated by centrifugation (Model: R23, Remi, Mumbai, India) at 3000 rpm for 30 min. The supernatant solution was ultrasonicated for 5 min prior to zeta potential analysis.

Bulk density (BD), apparent porosity (AP), and water absorption (WA) capacity of sintered samples were measured according to Archimedes principle (ASTM C372) using Mettler balance (AG 245, Mettler Toledo, Heuwinkelstrasse, Switzerland). On an average, three density measurements were performed for each sample in this study (±0·01 error) (Ganesh *et al* 2001, 2002b, 2003, 2004). XRD patterns were recorded on a Bruker (Karlsruhe, Germany) D8 advanced system using diffracted beam monochromated Cu K_α (0·15406 nm) radiation source. Relative phase compositions of samples were calculated from the respective peak height measurements (Cullity 1978). Crystalline phases were identified by comparison with PDF-4 reference data from International Centre for Diffraction Data (ICDD). To obtain quantitative information of various phases, the most intense peak of the individual phases was taken into consideration. The peak heights of all the phases were summed up and the percentage concentration of a particular phase was estimated from the ratio of the strongest peak of that phase to the sum of various phases present in a given system.

Microstructures of dense spinel ceramics were examined by SEM (JSM - 5410, JEOL, Tokyo, Japan) with an energy dispersive scanning attachment (Sigma 3·42 Quaser, Kevex, USA). The fracture surfaces of samples were examined after coating with carbon for conductivity. The mechanical properties evaluated were hardness (H) and flexural strength. Hardness data was collected using a microhardness tester (Leitz Wetzler, Germany) by holding a 137° indenter tip for 20 s under a load (P) of 10 kg on the mirror finished surface of the samples. Vickers hardness (H) was calculated as $H = P/2d^2$, d being the half-diagonal indentation impression. The flexural strength of the green and sintered samples was measured using a 3-point bending test (JIS-R1601). About 15 to 20 samples were tested per case and the results are presented as mean values (±0·01 error).

3. Results and discussion

The particle size distribution (PSD) and the average particle size (D_{50}) of raw materials, α-Al_2O_3, calcined caustic magnesia, and A-MAS powder obtained at 1400°C are presented in figure 2. It can be seen that A-MAS and alumina powders have uni-modal PSD and D_{50} values of 0·94 and 1·83 μm, respectively whereas MgO powder has a relatively wider PSD and $D_{50} = 5{\cdot}63\,\mu$m. A stoichiometric MAS with a D_{50} of 2 μm enabled reaching bulk density values $>3{\cdot}40$ g/cm^3 (i.e. >95% of the theoretical value) upon sintering at 1650°C for 1 h in our earlier studies (Ganesh *et al* 2001). In the present case, although the starting magnesia raw material has an apparently larger $D_{50} = 5{\cdot}63\,\mu$m, its specific surface area of ∼15 m^2/g indicates that its primary particles are finer. The measured average size is for the agglomerates, which tend to be destroyed during ball milling.

The X-ray diffraction patterns of the starting raw materials and of the MAS powders synthesized by solid state reaction at temperatures in the range of 1000° to 1400°C for 1 h from a stoichiometric mixture of alumina and magnesia are presented in figure 3. For comparison purposes, the XRD patterns reported in standard ICDD files for corundum (ICDD File No: 00–46–1212), periclase (ICDD File No: 00–45–946) and a stoichiometric MAS (ICDD File No: 00–21–1152) are also presented in this figure. Alumina and magnesia raw materials exhibit XRD lines corresponding to only corundum and periclase phases, respectively. Calcination for 1 h at 1000°C resulted in the formation of a small amount (∼10%) of spinel phase. The content of spinel phase

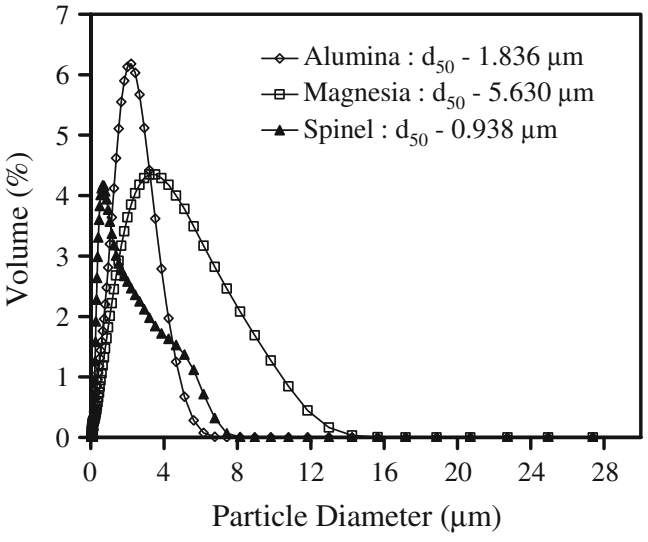

Figure 2. Particle size distributions of as purchased α-Al_2O_3 and calcined caustic MgO powders, and of the planetary ball milled $MgAl_2O_4$ spinel formed at 1400°C for 1 h.

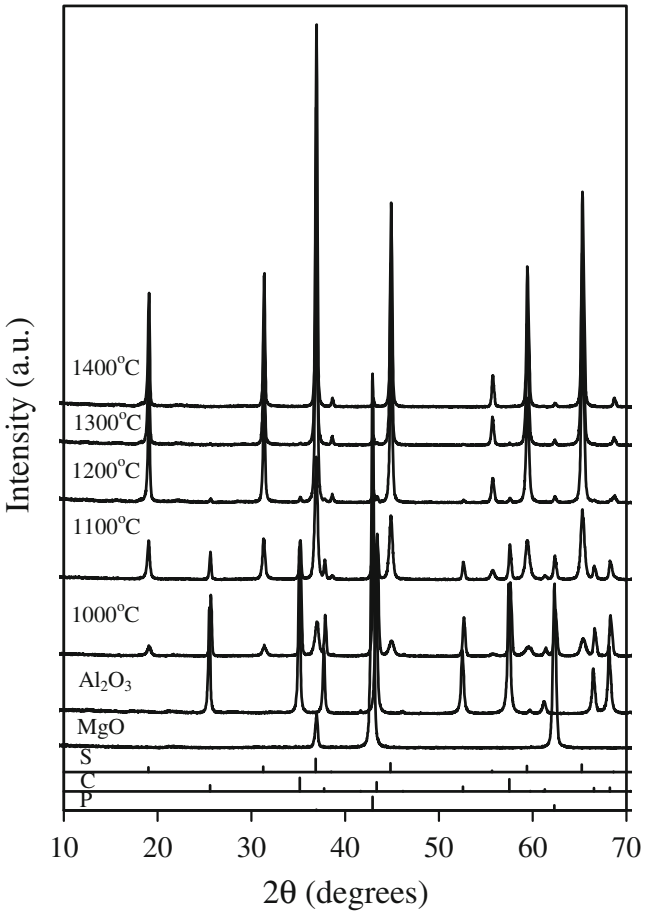

Figure 3. XRD patterns of as purchased α-Al_2O_3 and calcined caustic MgO, and of the $MgAl_2O_4$ spinel powders formed upon calcination for 1 h at temperatures between 1000 and 1400°C. P, periclase, ICDD File No: 00–45–946; C, corundum, ICDD File No: 00–46–1212; S, spinel, ICDD File No: 00–21–1152.

increased gradually with increasing heat treatment temperature, reaching about 45% at 1100°C, more than 80% at 1200°C, and about 94% at 1400°C (Ganesh *et al* 2001).

Temperatures higher than 1400°C were not used in order to keep a small amount of un-reacted alumina and magnesia raw materials in the calcined powder. It has been reported that partially spinelized (90–95%) powders possess higher reactivity during sintering when compared to un-calcined powders or fully spinelized powders at elevated temperatures (Ganesh *et al* 2001). This is mainly due to the higher calcination temperatures required for complete spinelization compared to partial spinelization, leading to the formation of hard agglomerated powders with low reactivity. The un-calcined powders cannot be sintered into dense MAS bodies because of the volume expansion associated with the spinel formation (Nakagawa *et al* 1995).

In our earlier studies, a single-phase MAS was identified when a stoichiometric mixture of α-Al_2O_3 and calcined caustic MgO was compacted by die-pressing (200 MPa) or by extrusion and calcined at 1350°C for 1 h (Ganesh *et al* 2001, 2002b, 2003, 2004, 2005, 2009). In the present study, the mixture of raw materials was consolidated by TIG (Bergström 1994) from organic-based suspensions containing 40 vol.%. The lower packing green density of the consolidates means higher diffusion paths of the species, and a heat treatment schedule of 1 h at 1400°C was required to reach a spinel content of about 95%. Formation of $MgAl_2O_4$ by the solid-state reaction of corundum and periclase is explained by the Wagner mechanism (Nakagawa *et al* 1995). The reaction proceeds by counter diffusion of the cations through the product layer, with oxygen ions remaining at the initial sites. To keep the electro-neutrality, $3Mg^{2+}$ diffuse toward the alumina side and $2Al^{3+}$ diffuse toward the magnesia side to form 3 moles of $MgAl_2O_4$. Therefore, shorter diffusion paths make the reaction between alumina and magnesia to occur faster. Powders with fine average particles size (i.e. 2 μm) can be mixed very intimately to accelerate the reaction. In the present case, although the starting magnesia raw material has an apparently larger $D_{50} = 5{\cdot}63\,\mu$m, its specific surface area of 15·15 m^2/g indicates that the primary particles are finer and the measured average size is for the agglomerates, which tend to be destroyed during ball milling.

Figure 4 shows the ζ behaviour of T-MAS powder under the influence of different concentrations of dispersing agents. It can be seen that the absolute ζ values decrease gradually with increasing amounts of added dispersants, reaching minimum of about -34 mV and -35 mV in the presence of 20 μL Duramax D-3005, or 35 μL TMAH per gram of powder, respectively followed by increasing trends for further added amounts of individual dispersants. The combination of a fixed amount of TMAH (35 μL per gram of powder) with varying amounts of Duramax D-3005, enabled developing higher ζ values, more suitable to electrostatically stabilized concentrated suspensions. According to DLVO theory (Lewis 2000) a high ζ-potential $> \pm 40$ mV is necessary to

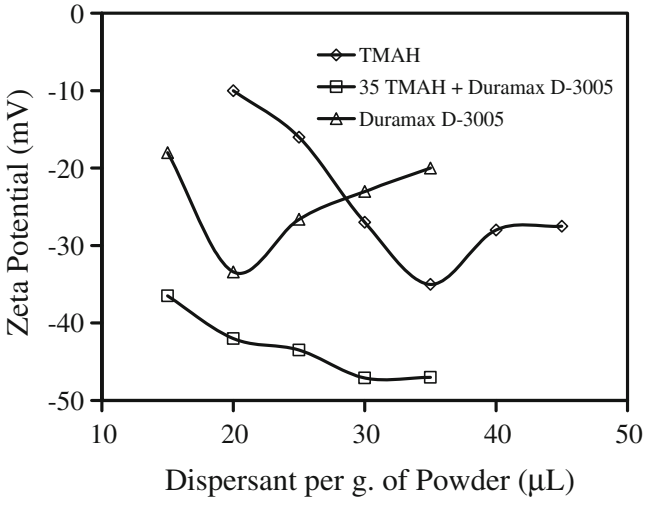

Figure 4. Change in zeta potentials of treated MAS powders in water as a function of dispersant concentration in the suspension.

Table 1. Slurry characteristics and properties of slip cast green MAS bodies.[†]

Sample	Solids loading (vol.%)	H_2O (mL)	TMAH (μL)	Duramax D-3005 (μL)	MAS powder (g)	Slurry viscosity at 140 s^{-1} (mPa.s)
SC-41	41	25·5	1834	1834	73·79	466·23
SC-42	42	25·0	1879·5	1879·5	75·18	577·64
SC-43	43	24·5	1924·2	1924·2	76·97	786·35
SC-44	44	24·0	1969·0	1969·0	78·76	821·91
SC-45	45	23·5	2013·7	2013·7	80·55	965·20

[†]Values were obtained as detailed in the experimental section.

Table 2. Properties of slip cast MAS ceramics (SC-41 to SC-45) sintered at 1600°C for 2 h and die-pressed sample (DP) sintered at 1650°C for 1 h.[†]

Sample	Green density (g/cm^3)	Green strength (MPa)	Bulk density (g/cm^3)	Apparent porosity (%)	Water absorption capacity (%)	Hardness (Hv or Kg/mm^2)	Flexural strength (MPa)
SC-41	1·722	9·246	3·435	1·341	0·407	674·61 ± 13·4	176·47 ± 15
SC-42	1·693	8·821	3·412	1·165	0·356	678·96 ± 26·1	144·99 ± 16
SC-43	1·648	8·123	3·364	2·013	0·622	668·87 ± 22·5	125·67 ± 12
SC-44	1·633	7·983	3·359	2·404	0·662	637·51 ± 13·7	113·94 ± 13
SC-45	1·623	7·832	3·356	3·034	0·785	655·89 ± 19·3	111·93 ± 11
DP	1·665	0·245	3·506	0·064	0·018	811·36 ± 18·63	173·03 ± 6·7

[†]Values were obtained as detailed in the experimental section.

prepare stable and high solids loaded aqueous suspensions required for near-net shape forming of ceramics (Parks and De Bruyn 1962; Pugh 1994). A repulsive force of enough magnitude is necessary between particles to overcome the Van der Waals attractive interactions that tend to hold them together forming agglomerates. Aqueous ceramic suspensions are stabilized normally either by adjusting the pH of the suspension away from the iso-electric point (pH_{iep}) of the powder (electrostatic stabilization) or by using polyelectrolytes as dispersing agents (electrosteric stabilization). Pure electrostatic stabilization usually requires higher absolute ζ values, which will increase the adlayer thickness around the particles, limiting again the achievement of high solids loading. Duramax D-3005 acts by electrosteric stabilization, enabling the preparation of stable and concentrated aqueous suspensions.

The surface of the MAS powder particles presents AlOH and MgOH groups. These hydroxyl groups dissociate into water and confer to the particles a surface charge according to reactions (1) and (2):

$$\left(MgAl_2O_4\right) - M - OH + H^+ \leftrightarrow M - OH_2^+$$

$$(\text{where } M = \text{Al and Mg}), \quad (1)$$

$$\left(MgAl_2O_4\right) - M - OH + -OH^- \leftrightarrow M - O^- + H_2O. \quad (2)$$

The as-synthesized powder exhibited a pH_{iep} in the range of 9–10 (between those of alumina and magnesia) (Parks and De Bruyn 1962), whereas the treated one presented a pH_{iep} at about 3 (results not shown). This shift in the pH_{iep} confirms the anionic nature of the adsorbed phosphate species. The surface hydroxyl groups play an important role in the formation of the protective layer against hydrolysis when the MAS powder is treated with H_3PO_4 and $Al(H_2PO_4)_3$. The chemisorption of these species onto the surface of the MAS powder particles can be described by reaction (3):

$$\text{Al}(OH)_3 + \text{Mg}(OH)_2 + H_3PO_4 + n\text{Al}(H_2PO_4)_3 \rightarrow (n+1)\,\text{Al}(H_2PO_4)_3 + \text{Mg}(H_2PO_4)_2 + 5H_2O. \quad (3)$$

The reaction occurs between $Al(OH)_3$ or $Mg(OH)_2$ and H_3PO_4. The $Al(H_2PO_4)_3$ is expected to perform only a seeding action as the $Al(OH)_3$ or the $Mg(OH)_2$ ultimately converts into $Al(H_2PO_4)_3$ or $Mg(H_2PO_4)_2$ by reacting with H_3PO_4 under the mild reaction conditions employed (Ganesh *et al* 2008c). It has been reported that ~1·1 mg $H_2PO_4^-$ is required to form a continuous single uni-molecular phosphate monolayer on a square meter surface of hydrated alumina-based materials (Ganesh *et al* 2008c). The measured BET surface area for the MAS powder of 3·98 m^2/g will only require about 4·38 mg per gram for providing a continuous protective layer. However, a higher concentration of 2·18 mg of $H_2PO_4^-$ ions in the form of H_3PO_4 and $Al(H_2PO_4)_3$ per square meter of MAS powder (i.e. 2·18 × 3·98 = 8·676 mg per g of powder) was used in the present work to ensure an effective coating of all MAS particles. The excess

unreacted phosphate was removed from the treated MAS powder surface by washing with absolute ethanol.

Table 1 reports the data concerning suspensions preparation and their characteristics including solids loading, water content, concentrations of dispersing agents TMAH and Duramax D-3005, amount of MAS powder and viscosity at $\dot{\gamma} = 140\,s^{-1}$. For simplicity purposes, different codes are given to samples, with SC standing for slip casting and numbers 41–45 denoting the solids volume fractions in the suspensions. A significant increase of the suspensions' viscosity with increasing solids loading can be observed, reaching a highest value of 965·20 mPa.s at 140 s^{-1} for the suspension containing 45 vol.% solids (SC-45). According to Janney *et al* (1998), 45 vol.% solids loading is high for certain powders, such as Ube E10 silicon nitride Starck, B10 silicon carbide, TOSOH TZ zirconias, and Baikowski high purity aluminas. In all these cases, the powders are exceedingly difficult to disperse because of their high specific surface areas.

The values of bulk density (BD), apparent porosity (AP), water absorption capacity (WA) and the hardness and flexural strength of the SC-41 to SC-45 and the one obtained by the die-pressing of freeze-dried granules (DP) sintered for 1–2 h at 1550–1650°C are presented in table 2 together with green density and 3-point bend strength values. It can be seen that the green density of slip cast bodies decreased gradually with increasing solids loadings from 1·722 g/cm^3 (48·92% of theoretical density (TD)) for the sample SC-41, to 1·623 g/cm^3 (45·34% of TD) for the sample SC-45. However, these values are well comparable with the one noted for die-pressing of freeze-dried granules (1·665 g/cm^3, 46·50% of TD). Often, when there is a coagulation trend, lower viscosity suspensions undergo better compaction upon slip casting as powder particles can more easily slid over each other leading to better interlocking and to consolidate with high green density and green strength. This seems to have occurred in the present study since the measured green strength values show the same decreasing trend observed for green density.

It can be seen that BD gradually decreased from about 3·435 g/cm^3 to 3·356 g/cm^3 with solids loading increasing from 41 to 45 vol.% upon sintering at 1600°C for 2 h. This decrease is accompanied by concomitant and consistent increases in both AP and WA capacity values. Sintered SC-41 to SC-43 samples exhibit values of AP and WA capacity of 2·013% and 0·622%, respectively whereas the SC-44 and SC-45 samples are clearly more porous, with the SC-45 one presenting an apparent porosity of about 3·034% and a water absorption capacity of about 0·785%. As can be seen from data in table 2 BD of the sintered materials is strongly dependant on green density of consolidates, which in turn is a function of the viscosity of the suspension. The stoichiometric $MgAl_2O_4$ spinel consists of 71·8 wt.% Al_2O_3 and 28·2 wt.% MgO (theoretical density, TD = 3·58 g/cm^3, ICDD File No: 00–021–1151, *Fd3m* structure). The die-pressed (DP) sample exhibited a BD value of 3·506 g/cm^3, apparent porosity of 0·064% and a water absorption capacity of 0·018% upon sintering at 1650°C for 1 h. The difference noted in the sintered properties of slip cast samples and the die-pressed one could be attributed to the difference in the sintering temperatures. It is known that the rate of sintering increases exponentially with increase in temperature.

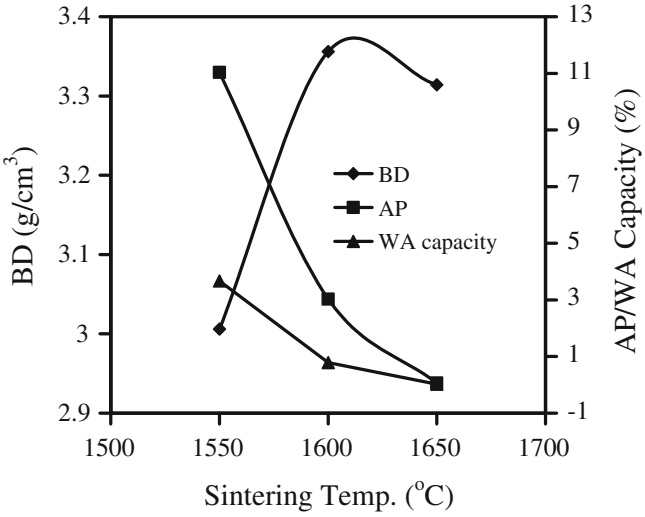

Figure 5. Evolution of bulk density (BD), apparent porosity (AP) and water absorption (WA) capacity of $MgAl_2O_4$ spinel consolidated by slip casting route using aqueous suspension containing 45 vol.% solids and sintered for 2 h at 1550–1650°C.

The evolution of BD, AP and WA capacity of SC-45 sintered for 2 h through 1550° and 1650°C is presented in figure 5. BD gradually increased from 3·01 g/cm^3 to 3·37 g/cm^3 when the sintering temperature changed from 1550°C to 1600°C. However, a lower value of BD (3·32 g/cm^3) was measured with a further increase in sintering temperature, against the expectations, but a good consistency is observed between the values of AP and WA capacity, and of BD. Sintering for 2 h at 1550°C resulted in AP and WA capacity values of about 11% and 3·7%, respectively which then approached zero with further increase in sintering temperature to 1650°C. One reason for the slight decrease in the BD for sintering temperatures above 1600°C could be ascribed to the increased grain size in the samples or to any volume expansion associated with the spinel formation from the remaining unreacted powders (Nakagawa *et al* 1995).

As can be seen from table 2, there is a decreasing trend in the hardness and flexural strength values of slip cast MAS samples sintered for 2 h at 1600°C with solids loading increasing from 41 to 45 vol.%. The sample SC-41 exhibits hardness and flexural strength values of about 674·61 ± 13·4 kg/mm^2 and of 176·47 ± 15 MPa, while those of sample SC-45 are 655·89 ± 19·3 kg/mm^2 and 111·93 ± 11 MPa, respectively. A gradual decrease in the hardness and flexural strength with decreasing BD is evident. The higher porosity fractions of less dense MAS ceramics are responsible for their lower hardness and flexural strength values. The

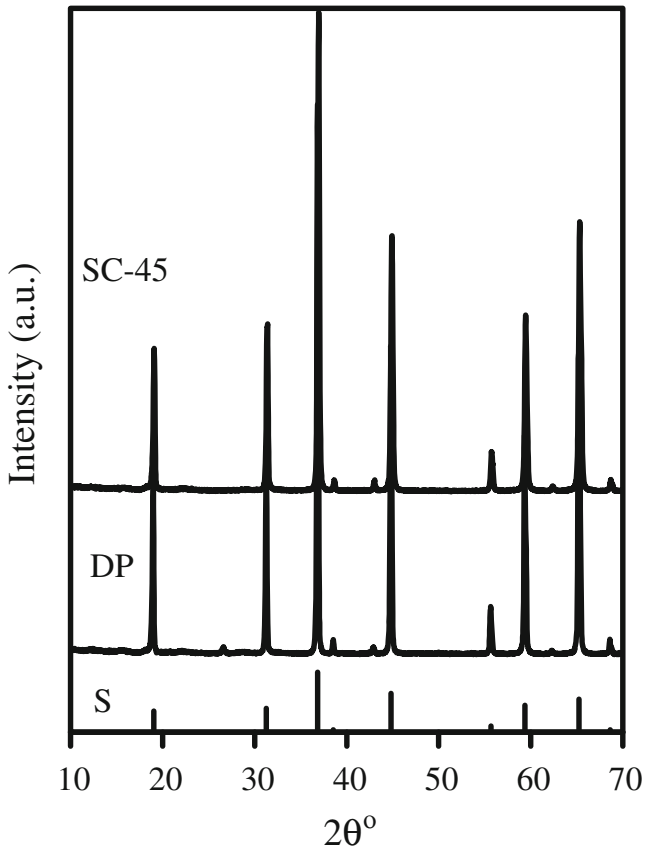

Figure 6. XRD patterns of DP and SC-45 consolidated bodies sintered for 1 h at 1650°C and 2 h at 1600°C, respectively. S, spinel, ICDD File No. 00–21–1152.

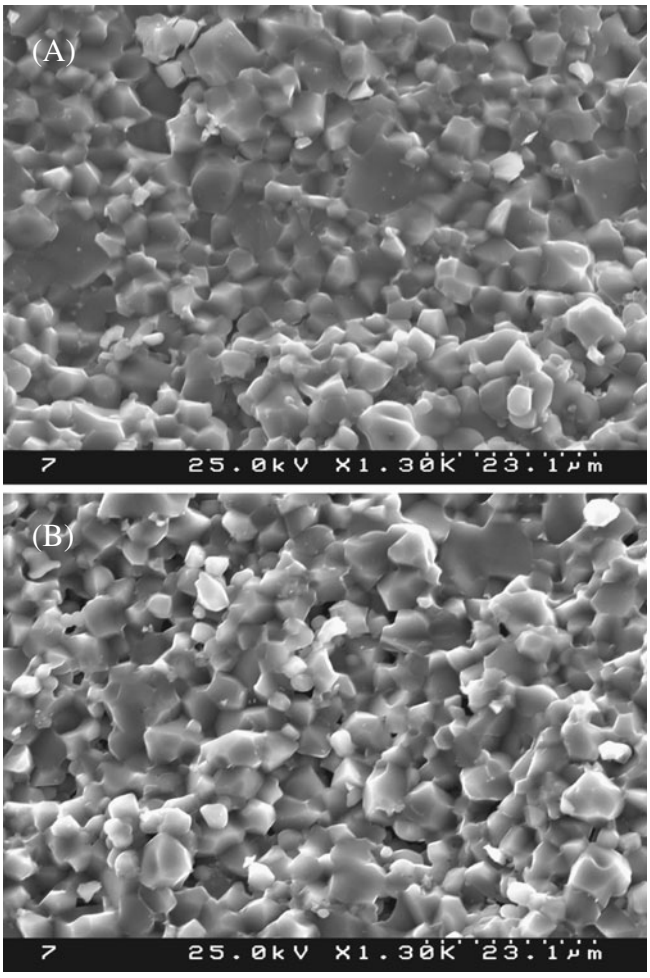

Figure 7. SEM micrographs of fracture surfaces of DP and SC-45 consolidated bodies sintered for 1 h at 1650°C and 2 h at 1600°C, respectively.

DP sample upon sintering at 1650°C for 1 h exhibited a hardness of 811·36 ± 18·63 Hv and 3-point bend strength of 173·03 ± 6·7 MPa. Interestingly, the mechanical properties of slip cast samples are comparable with those of DP. Bhaduri and Bhaduri (2002) reported a hardness of 779 kg/mm^2 for a nanocrystalline dense MAS consolidated by aqueous slip casting, followed by cold isostatic pressing (CIPing) at 275 MPa for 10 min, and then by hot isostatic pressing (HIPing) at 1300°C for 4 h. The hardness and flexural strength values obtained in the present study without using such heavy equipments are comparable to those reported in the literature for MAS ceramics (Porter *et al* 1977; White and Kelkar 1992).

X-ray diffraction patterns of DP and SC-45 sintered for 1 h at 1650°C and 2 h at 1600°C, respectively exhibit peaks corresponding to only stoichiometric $MgAl_2O_4$ spinel phase (figure 6). For comparison purposes, the XRD pattern reported in standard ICDD files for stoichiometric MAS (ICDD File No. 00-21-1152) is also presented in this figure. According to the phase diagram of binary MgO–Al_2O_3, $MgAl_2O_4$ is the only phase formed at temperatures up to 1600°C. At this temperature, the solid solubility of MgO and Al_2O_3 in the spinel is 2 and 6%, respectively. On increasing the firing temperature to 1700°C, the solubility in the spinel increases to 3·0 and 10·0%, respectively (Ganesh *et al* 2008a). This solid solubility helps to explain why minor phases could not be identified by XRD in the samples sintered above 1600°C.

The SEM micrographs of DP and SC-45 samples sintered at 1650°C for 1 h, and at 1600°C for 2 h, respectively are presented in figures 7(a) and 7(b). It can be seen that both samples appear relatively dense. Some small intragranular pores are observed in the sample DP, while few larger intergranular pores are apparent in the SC-45 sample. The first kind of fine pores might be due to porosity present in the freeze dried granules, while the larger ones in the sample SC-45 might be attributed to pull out of grains during fracture or to pores entrapped in the green consolidates. Nevertheless, both samples have similar microstructures with equi-axed grains which are tightly packed. These results are well comparable with those reported for the MAS materials in the literature (Ganesh *et al* 2003).

4. Conclusions

Stoichiometric $MgAl_2O_4$ spinel (MAS) powder could be prepared from a mixture of α-Al_2O_3 and calcined caustic MgO compacted by temperature-induced gelcasting (TIG) using azeotropic mixture of methyl-ethyl-ketone and ethanol in 60:40 volume ratio followed by calcination at 1400°C for 1 h. Orthophosphoric acid and aluminium dihydrogen phosphate enabled to achieve an extensive degree of surface passivation of the MAS particles and increase by 50% (from 30 vol.% to 45 vol.%) the solids loading of this powder in aqueous suspensions making them suitable for slip casting. This study demonstrates the near-net shape fabrication of $MgAl_2O_4$ spinel ceramics from aqueous suspensions containing 41–45 vol.% solids loading. The die-pressed and slip cast samples exhibited comparable properties upon sintering.

Acknowledgements

Author thanks Dr G Sundararajan, Director, ARCI, for his valuable suggestions to this work. Thanks are also due to Prof. J M F Ferreira, Department of Ceramics and Glass Engineering, CICECO, University of Aveiro, Aveiro, Portugal, for his technical inputs to the manuscript. Author also expresses his gratitude to Dr S M Olhero, Senior Researcher, CICECO, University of Aveiro, Portugal, for measuring green data slip cast MAS samples.

References

Angappan S, Berchmans L J and Augustin C O 2004 *Mater. Lett.* **58** 2283

Baudin C, Martinez R and Pena P 1995 *J. Am. Ceram. Soc.* **78** 857

Belding J H and Letzgus E A 1976 U.S. Patent No. 3 950 504

Bergström L 1994 U.S. Patent 534053223

Bhaduri S and Bhaduri S B 2002 *Ceram. Int.* **28** 153

Cullity B D 1978 *Elements of XRD* (Reading, MA: Addison-Wesley) 2nd ed.

Ganesh I 2009 *Int. J. Appl. Ceram. Technol.* **6** 89

Ganesh I, Bhattacharjee S, Saha B P, Johnson R and Mahajan Y R 2001 *Ceram. Int.* **27** 773

Ganesh I, Bhattacharjee S, Saha B P, Johnson R, Rajeshwari K, Sengupta R, Ramanarao M V and Mahajan Y R 2002a *Ceram. Int.* **28** 245

Ganesh I, Srinivas B, Johnson R, Saha B P and Mahajan Y R 2002b *Br. Ceram. Tr.* **101** 247

Ganesh I, Srinivas B, Johnson R, Rao G V N and Mahajan Y R 2003 *Br. Ceram. Tr.* **102** 119

Ganesh I, Srinivas B, Johnson R, Saha B P and Mahajan Y R 2004 *J. Eur. Ceram. Soc.* **24** 201

Ganesh I, Teja K A, Thiyagarajan N, Johnson R and Reddy B M 2005 *J. Am. Ceram. Soc.* **88** 2752

Ganesh I, Olhero S M, Rebelo A H and Ferreira J M F 2008a *J. Am. Ceram. Soc.* **91** 1905

Ganesh I, Thiyagarajan N, Jana D C, Barik P and Sundararajan G 2008b *J. Am. Ceram. Soc.* **91** 3121

Ganesh I, Olhero S M, Branca A A, Correia M R, Sundararajan G and Ferreira J M F 2008c *Langmuir* **24** 5359

Ganesh I, Olhero S M, Rebelo A H and Ferreira J M F 2009 *J. Am. Ceram. Soc.* **92** 350

Graule T J, Baaber F H and Gauckler J L 1994 *Cfi/Ber. DKG* **71** 317

Green K E, Hastert J L and Roy D W 1989 *Proc. Soc. Photo-Opt. Instrum. Eng.* **A90–34551** 14

Harris D C 1992 *Infrared window and dome materials* (Washington: SPIE) p. 32

Hing P 1976 *J. Mater. Sci.* **11** 1919

Janney M A, Nunn S D, Walls C A, Omatete O O, Ogle R B, Kirby G H and McMillan A D 1998 *Gelcasting*; in *The handbook of ceramic engineering* (ed.) M N Rahman (New York: Marcel Dekker) pp 1–15

Kosmac T, Novak S and Sajko M 1997 *J. Euro. Ceram. Soc.* **17** 427

Kumar P and Sandhage K H 1998 *Near net-shaped magnesium aluminate spinel by the oxidation of solid magnesium-bearing precursors*, TMS Outstanding Student Paper Contest Winner-1998 (Columbus: Department of Materials Science and Engineering, The Ohio State University)

Lewis J A 2000 *J. Am. Ceram. Soc.* **83** 2341

Nakagawa Z E, Enomoto N, Yi I S and Asano K 1995 *UNITECER'95 Proceedings* (Tokyo) p. 379

O'Driscoll M 1997 *IM Fused Minerals Review* **6** 44

Parks G A and De Bruyn P L 1962 *J. Phys. Chem.* **66** 967

Patel P J, Gilde G A, Dehmer P G and McCauley J W 2000 *The AMTIAC Newsletter*

Porter D F, Reed J S and Lewis D 1977 *J. Am. Ceram. Soc.* **60** 345

Pugh R J 1994 *Surface and colloidal chemistry in advanced ceramic processing* (New York: Surfactant Sciences Series) **Vol. 51**

Roy D W 1998 *History of spinel development*, Presented to DARPA/ARL, Transparent Armor Workshop (Annapolis, MD)

Sainz M A, Mazzoni A, Aglietti E and Caballero A 1995 *Proceedings UNITESR'95* 387

Shimizu Y, Arai H and Seiyama T 1985 *Sens. Actuator* **7** 11

Urita Y, Yamaguchi K, Takita I, Furuta K and Natsuo Y 1993 *Taikabutsu* **45** 664

Wei G C 2005 *J. Phys. D: Appl. Phys.* **38** 3057

White K W and Kelkar G P 1992 *J. Am. Ceram. Soc.* **75** 3440